Structural Characterization of the Native NH_2-Terminal Transactivation Domain of the Human Androgen Receptor: A Collapsed Disordered Conformation Underlies Structural Plasticity and Protein-Induced Folding†

Derek N. Lavery‡ and Iain J. McEwan*

School of Medical Sciences, Institute of Medical Sciences, University of Aberdeen, Foresterhill, Aberdeen AB25 2ZD, United Kingdom

Received November 7, 2007; Revised Manuscript Received January 31, 2008

ABSTRACT: The androgen receptor (AR) mediates the action of the steroid hormones testosterone and dihydrotestosterone. The protein contains two globular α-helical domains responsible for binding hormone and DNA. In contrast, the N-terminal domain is less well structurally defined and contains the main determinants for receptor-dependent transactivation, termed AF1. Previously, we have shown this region has the propensity to form α-helix structure. Significantly, the binding of specific protein targets or a natural osmolyte resulted in a more protease resistant conformation for the AF1 domain, consistent with an increase in conformational stability. Computational and experimental analyses were used to investigate the conformational properties of the native AF1 domain. This region of the receptor is predicted to contain significant regions of natural disordered structure, when analyzed by amino acid composition, PONDR (Predictor of Natural Disordered Regions), RONN (Regional Order Neural Network), and GlobPlot, but is grouped with ordered proteins on a charge−hydropathy plot. The binding of a hydrophobic fluorescence probe, 8-anilinonaphthalene-1-sulfonic acid (ANS), together with size-exclusion chromatography suggests that native AR-AF1 exists in a collapsed disordered conformation, distinct from extended disordered (random coil) and a stable globular fold. This state has also been described as premolten or molten globule-like. These findings are discussed in terms of the functional importance of the intrinsic plasticity of the AF1 domain.

The androgen receptor (AR)[1] is a ligand-activated transcription factor that mediates the actions of the steroid hormones testosterone and dihydrotestosterone. Three-dimensional structures, derived from modeling or X-crystallography, are available for the isolated ligand binding domain (LBD) bound with agonists (*1–3*) and antagonists (*4*) or complexed with peptides derived from coregulatory proteins (see ref *5*). Similarly, atomic-resolution structural information is available for the isolated DNA-binding domain (*6*). The N-terminal domain (NTD), in contrast, appears disordered and structurally flexible and participates in multiple protein–protein interactions (reviewed in ref *7*). The major transactivation function of the AR has been mapped to the NTD of the protein by deletion and point mutations (*8–10*). This domain (amino acids 142−485), defined as AF1, can activate a reporter gene in both mammalian and yeast cells when fused a heterologous DNA binding domain and retains at least 65% of the transactivation activity of the full-length NTD under these conditions (*9, 12*). We have previously reported the interaction of AR-AF1 with the large subunit of TFIIF, termed RAP74 (*11*), and the p160 coactiavtor protein SRC-1a and have mapped the receptor binding sites to the N- and C-terminal regions of RAP74 and the CTD of SRC-1a (*12*).

It has become increasingly evident that many proteins are composed of regions with limited structure and high levels of intrinsic disorder (*13, 14*). Recently, multiple acidic transcription factors have been shown to contain regions of limited structure such as VP-16 (*15–19*), p53 (*20*), NF-κB (*21*), CREB (*22–24*), and the glucocorticoid receptor AF-1, or tau-1, domain (GR-AF1/τ1), a member of the steroid hormone receptor (SHR) subfamily of nuclear receptors (*25, 26*). One of the best studied, CREB, shows induced folding of the transactivation domain concomitant with phosphorylation and target protein binding (*22–24, 27*). "Induced" or "coupled" binding or folding has many advantages over more

† This work was funded by a project grant from The Association for International Cancer Research (03-127). D.N.L. was funded by a Ph.D. studentship from the Association of International Cancer Research.

* To whom correspondence should be addressed: School of Medical Sciences, Institute of Medical Sciences, University of Aberdeen, Foresterhill, Aberdeen AB25 2ZD, Scotland, United Kingdom. Telephone: +44(0)1224-555807. Fax: +44(0)1224-555844. E-mail: iain.mcewan@abdn.ac.uk.

‡ Present address: Androgen Signalling Laboratory, Department of Oncology, Imperial College London, London, U.K.

[1] Abbreviations: AF-1, activation function 1; ANS, 8-anilinonaphthalene-1-sulfonic acid; AR, androgen receptor; BSA, bovine serum albumin; CBP, CREB binding protein; CDF, cumulative distribution function; CH, charge−hydropathy; CTD, C-terminal domain; DND, DNA binding domain; ERα, estrogen receptor α; GR, glucocorticoid receptor; GST, glutathione *S*-transferase; K_{av}, distribution coefficient; α-LA, α-lactalbumin; LBD, ligand binding domain; MID, middle domain; NTD, N-terminal domain; PBS, phosphate-buffered saline; PONDR, predictor of natural disordered structure; PSA, prostate-specific antigen; RAP30/74, RNA polymerase II-associated protein 30/74; RONN, regional order neural network; SHR, steroid hormone receptor; SRC, steroid receptor coactivator; TCA, tricarboxylic acid; TMAO, trimethylamine *N*-oxide; V_c, column volume; V_e, elution volume; V_o, void volume.

10.1021/bi702221e CCC: $40.75
Published on Web 02/20/2008

structurally rigid protein–protein interactions, including achieving specificity without the need for high affinity, multiple structural conformers, and therefore the potential for binding multiple target proteins and large interacting surfaces (*13*). The N-terminal domains of SHRs have been reported to be highly unstructured using a variety of spectroscopic techniques (reviewed in ref *7*). Furthermore, NTD/AF1 domains of the GR and AR appear to "fold" into a more ordered and globular conformation when incubated with the natural osmolyte trimethylamine *N*-oxide (TMAO) and organic solvent trifluoroethanol (TFE) (*25, 26, 28, 29*). Significantly, for the AR, the GR, and estrogen (ER) and progesterone (PR) receptors, an α-helical conformation can be achieved in NTD/AF1 through the binding of coregulatory proteins such as TBP (*30, 31*), TFIIF (*32*), and JDP-2 (*33*).

Given the importance of the AF1 domain for AR action, it is vital to understand the native conformation and folding properties of this domain. We investigated protein conformation under native conditions and in the presence of different binding partners, using a range of methods, including fluorescence spectroscopy, size-exclusion chromatography, protein–protein interactions, and limited proteolysis studies. We have also compared the findings of different computational methods for predicting regions of intrinsic disorder. The outcomes of this analysis extend earlier studies showing that AR-NTD/AF1 contains significant sequences of natural disordered structure and reveals the possibility that native AR-AF1 exists in an intermediate folded state. Using binding of the hydrophobic fluorescent probe 8-anilino-1-naphthalenesulfonic acid (ANS), which does not fluoresce free in solution, we show that this domain unfolds in a noncooperative manner when titrated with increasing molar concentrations of urea, similar to molten globule proteins. We have characterized the hydrodynamic properties of isolated AR-AF1 using size-exclusion chromatography. These results indicate that in a native state AR-AF1 has structural features distinct from those of globular and random-coil conformations and has properties similar to those of pre- or molten globule folded intermediates. Taken together, the results allowed us to refine our model for protein-induced folding of AR-AF1 and transactivation function.

EXPERIMENTAL PROCEDURES

Plasmid Construction. The plasmids containing the AF1 domain (amino acids 142–485) of the human AR tagged with histidine and GST and histidine-tagged RAP74 (full-length and domains) have been described previously (*29*).

Protein Expression and Purification. Histidine-tagged AR-AF1 (amino acids 142–485), full-length RAP74 (amino acids 1–517), RAP74-NTD (amino acids 1–136), and RAP74-MID (amino acids 258–356) were expressed in *Escherichia coli* strains BLR(DE3) and BL21(pLysS) for 1.5–2 h by induction with 1 mM isopropyl β-D-thiogalactoside at 37 °C in LB or 2×TY medium. Bacterial cells were pelleted by centrifugation, resuspended in buffer A [20 mM Tris-HCl (pH 7.9), 50 mM NaCl, 1 mM EDTA, 1 mM phenylmethanesulfonyl fluoride, and 1 mM dithiothreitol], and stored at −80 °C. Cell lysis was achieved by freezing and thawing and addition of lysozyme (0.5 mg/mL) at 4 °C. Proteins were purified from the soluble fraction by Ni^{2+}-agarose affinity chromatography (Qiagen). RAP74-NTD is insoluble under these conditions and was purified from inclusion bodies by denaturation with 8 M urea and subsequent Ni^{2+}-agarose affinity chromatography (Qiagen). GST and the GST−AR-AF1 fusion protein were expressed at 25 °C in BLR(DE3) or BL21(pLysS) *E. coli* cells for 3 h by induction with 0.1 mM isopropyl β-D-thiogalactoside in 2×TY medium. All proteins (excluding full-length and domains of RAP74) were dialyzed extensively against 25 mM HEPES (pH 7.9), 100 mM sodium acetate, 5% glycerol, and 1 mM dithiothreitol at 4 °C. RAP74 (excluding RAP74-NTD) proteins were dialyzed against 25 mM HEPES (pH 7.9), 250 mM sodium acetate, 5% glycerol, and 1 mM dithiothreitol at 4 °C. RAP74-NTD was dialyzed against the buffer described above but in a stepwise fashion, reducing the concentration of urea in molar amounts at hourly stages. Proteins were assessed for purity by SDS−PAGE, and concentrations were estimated using known BSA concentrations using Bradford reagent (Bio-Rad). Aliquots of protein were snap-frozen in liquid N_2 and stored at −80 °C until they were used. A synthetic peptide corresponding to amino acids 1102–1142 of SRC1a was synthesized by I. Davidson (University of Aberdeen).

Partial Proteolysis. To examine the tertiary structure of recombinant proteins, proteins were challenged with proteolytic enzymes. Fifty picomoles of recombinant protein was diluted in proteolysis buffer [25 mM HEPES (pH 7.9), 0.2 mM EDTA, 5 mM $MgCl_2$, 20 mM $CaCl_2$, 60 mM KCl, and 10% glycerol] and incubated in the absence or presence of 2 M TMAO or a 5-fold molar excess of binding partner on ice for 30 min in a total volume of 25 μL. Protein complexes were then challenged with trypsin (0.4 ng/μL) or chymotrypsin (2 ng/μL) over a series of time points (from 0 to 20 min) at room temperature or 30 °C. To keep protein concentrations equal, a 5-fold molar excess of a AF1 noninteracting polypeptide (RAP74-MID) was added where necessary. Reactions were stopped by addition of 2× SDS sample buffer, and samples were heated at 75 °C for 5 min. Samples were resolved by SDS−PAGE on a 12.5 or 15% gel and fragments generated analyzed by silver staining.

Bioinformatic Analysis. To assess the relative disorder of AR-AF1, AR-NTD, and AR-LBD, we used amino acid content bias (*34, 35*), together with the PONDR (Predictor of Natural Disordered Regions) algorithm (www.PONDR.com, Molecular Kinetics) (*35, 36*), charge−hydropathy (CH) plots (www.PONDR.com, Molecular Kinetics) (*37*), GlobPlot (http://globplot.embl.de) (*38*), RONN (Regional Order Neural Network, www.strubi.ox.ac.uk/RONN) (*39*), and FoldIndex (http://bip.weizmann.ac.il/fldbin.findex) (*40*). These algorithms are readily accessible through the relevant websites. The cumulative distribution function (CDF), a plot of the PONDR score versus the cumulative fraction of residues, and CH are binary predictors that classify proteins as "mostly" disordered or ordered on the basis of analysis of the primary amino acid sequence and score propensity for an amino acid to be in an ordered or disordered state. RONN is a neural trained network based on the alignment of the test sequence(s) against a data set of known ordered and disordered sequences. FoldIndex is a simple tool for predicting whether a polypeptide sequence is intrinsically folded or unfolded and is based a consideration of the charge and hydropathy of each residue. For each predictor, the default settings were used.

ANS Fluorescence Spectroscopy. Fluorescence studies with the hydrophobic probe 8-anilinonaphthalene-1-sulfonic acid (Fluka) were performed essentially as previously reported (*41, 42*) using a Shimadzu RF-1501 spectrofluorophotometer. Excitation and emission band widths were 10 nm, and the cuvette path length was 1 cm. To study the molten globule characteristics of AR-AF1, ANS binding to AR-AF1 was studied after excitation at 370 nm. The emission spectra were recorded over a wavelength range of 400–600 nm. For unfolding studies, 1 μM AR-AF1, BSA, or α-lactalbumin (α-LA) was incubated with ANS (50 μM) in PBS or a PBS/urea mixture (0.25–6 M) for 30 min at room temperature in the dark. Fluorescence measurements were performed at an excitation wavelength of 370 nm and an emission wavelength of 480 nm. Experiments were performed at least three times, and data points were averaged. Data are presented as the ratio of peak urea-titrated fluorescence (F) to peak native fluorescence (F_0). All measurements were corrected for both buffer and background (nonbound) ANS fluorescence.

Gel Filtration Analysis of AR-AF1. To examine the native molecular mass, structural characteristics, and hydrodynamic radius of AR-AF1, gel filtration chromatography was used. AR-AF1 was resolved on a column of Superose-6 gel medium under the control of an Äkta prime plus chromatography system (Amersham Biosciences). All buffers and gel media were chilled to 4 °C, vacuum-filtered (0.2 μm pore size), and degassed before being used. The column was equilibrated with 1−2 column volumes of running buffer (PBS, pH 7.5). A flow rate for subsequent separations was 0.5 mL/min (or 16.9 cm/h), and 1 mL fractions were collected with an automated fraction collector. During each run, fractions were monitored by UV absorbance at 280 nm. The column was calibrated with blue dextran and low-molecular mass standard proteins albumin, ovalbumin, chymotrypsinogen A, and ribonuclease A (Amersham Biosciences) in running buffer at a final concentration of 5 mg/mL, filter-sterilized (0.2 μm pore size), and applied to the column by manual injection. Runs for each protein were performed on at least three separate occasions, and the average elution volumes (V_e) for albumin, ovalbumin, chymotrypsinogen A, and ribonuclease A was measured to be 57.5 ± 2.9, 60.7 ± 1.2, 65.2 ± 2.4, and 67.3 ± 0.6 mL, respectively. The column volume (V_c) was calculated to be 68 mL and the gel phase distribution coefficient (K_{av}) calculated for each protein standard using the relationship $K_{av} = (V_e - V_o)/(V_c - V_o)$, and the values were plotted against the logarithm of protein standard molecular masses to generate a calibration curve for the column. The void volume (V_o) was determined using blue dextran (~2000 kDa) and equal to 32 ± 0.5 mL. A calibration curve was also generated relating the molecular mass and the hydrodynamic, or Stokes radius, of standard proteins. To determine the biophysical values of AR-AF1, purified protein was passed through 0.2 μm filters and a volume of 1 mL (representing ~1.5% of V_c) manually injected into the system. The V_e and K_{av} values were calculated and integrated into standard curves to determine both the apparent molecular mass and Stokes radius. AR-AF1 elution profiles were determined on four separate occasions and values averaged. Furthermore, eluted proteins were precipitated with 20% (v/v) TCA, analyzed by SDS−PAGE, and visualized by Coomassie blue staining.

RESULTS

Induced Folding of AR-AF1 upon Protein–Protein Interactions. Previously, we have shown that AR-AF1 adopts a more α-helical conformation upon binding the CTD of the large subunit of the general transcription factor TFIIF (RAP74-CTD) or in the presence of the chemical chaperone TMAO (*32*). This has led to a model in which protein folding and protein–protein interactions are dynamically coupled (*7*). To extend these studies for different binding partners, the sensitivity to protease challenge was measured using purified recombinant AR-AF1 and RAP74 polypeptides expressed in *E. coli* together with a peptide derived from the coactivator SRC-1a. Native AR-AF1 was rapidly digested by protease treatment, with full-length protein completely digested by 10 to 15 min with trypsin and by 2 min with chymotrypsin, resulting in a stable fragment representing GST (Figure 1 and data not shown). Incubation with the natural osmolyte TMAO induces a more protease resistant conformation, with the full-length polypeptide (65 kDa) significantly protected from both trypsin (Figure 1A, top panel) and chymotrypsin (Figure 1B, top panel) digestion. A number of intermediate fragments, the most notable at 55 kDa, also appear to be more stable in the presence of TMAO with both proteases (data not shown). The reduced level of proteolysis was not the result of impaired enzyme activity in the presence of TMAO (*29, 43*). These changes are consistent with induced folding and increased stability of AR-AF1. To investigate this further and to analyze the effect on conformation of different target proteins binding to AR-AF1, the sensitivity of AF1−protein complexes to partial proteolysis was measured. Purified AR-AF1 was incubated with a 5-fold molar excess of RAP74-NTD or SRC1a box B peptide (amino acids 1102–1142) on ice for ~30 min. To keep protein concentrations equal, a non-AR-AF1 interacting protein, RAP74-MID (see ref *12*), was added to control reaction mixtures. Preformed complexes were challenged with trypsin or chymotrypsin for time points up to 20 min at 30 °C and subsequently resolved by SDS−PAGE and fragments identified by silver staining. Panels A and B of Figure 1 show that, similar to that of TMAO, binding of RAP74-NTD (middle panel) or a 40-amino acid peptide from SRC-1a (bottom panel) specifically resulted in a reduced level of proteolysis of full-length AR-AF1 by both trypsin and chymotrypsin. The noninteracting protein, RAP74 middle domain (MID), which was used to keep the total protein concentration constant, failed to alter the sensitivity of AR-AF1 to partial proteolysis. Similar results have been obtained for full-length RAP74 or RAP74-CTD (ref *29* and data not shown). These results support the hypothesis that different protein–protein interactions are capable of inducing a more folded, protease resistant, conformation in the AR-AF1 transactivation domain.

Bioinformatics Analysis of the AR-AF1 Domain. Recent years have seen an increased interest in proteins that contain regions or whole domains of natural disordered structure. A number of predictive algorithms for intrinsically disordered sequence are now available, which use different physiochemical properties, such as amino acid composition, flexibility, hydropathy, or charge. To investigate the conformation of native AR-AF1 more comprehensively, we have used the trained predictors PONDR, RONN, and GlobPlot and

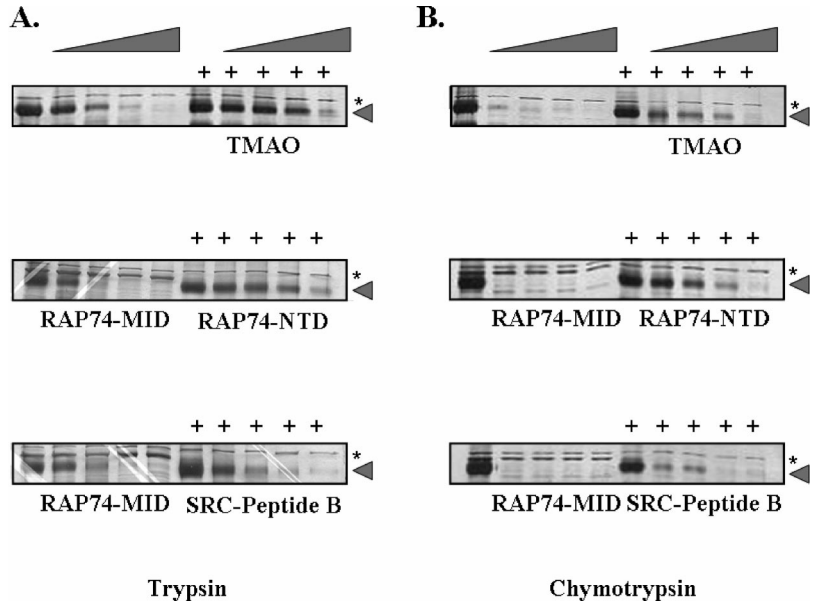

FIGURE 1: Partial proteolysis of AR-AF1 in the absence and presence of the natural osmolyte TMAO or specific protein–protein interactions. Panels A and B represent partial digestion of GST−AR-AF1 with trypsin (0.4 ng/μL) and chymotrypsin (2 ng/μL), respectively: (top) GST−AR-AF1 (50 pmol) in the absence (lanes 1–5) or presence (+, lanes 6–10) of TMAO digested with trypsin (0, 5, 10, 15, and 20 min) or chymotrypsin (0, 2, 5, 10, and 20 min) and (middle and bottom) GST−AR-AF1 (50 pmol) digested with trypsin (0.4 ng/μL) or chymotrypsin (2 ng/μL) for increasing time points, in the presence of a noninteracting protein, RAP74-MID (lanes 1–5), or a specific binding partner: (middle) RAP74-NTD (+, lanes 6−10) and (bottom) SRC-Peptide B (+, lanes 6–10). In all cases, lanes 1 and 6 represent undigested GST−AR-AF1 (time zero). Gels were stained with silver, and the full-length AR-AF1 polypeptide is indicated with the arrowhead; asterisks denote nonspecific bacterial proteins.

the nontrained algorithm FoldIndex to examine the structural organization of the human AR (Figure 2). PONDR (score above 0.5), RONN (score above 0.5), and GlobPlot (positive slope of curve) all predict extensive regions of natural disordered structure within the AR-NTD and AF1: amino acids 35–165, 186–234, 265–348, and 365–386 (Figure 2B−D). FoldIndex (negative score) identified two of these regions: amino acids 35−137 and 193–217 (Figure 2E). All four alogorithms correctly predicted the expected folded globular structure for the AR-LBD (Figure 4B−E), although only RONN and GlobPlot identified the structured DBD and likely unstructured hinge region between the DBD and LBD (Figure 2C,D). Taken together, this analysis strongly suggests that the AR-NTD contains significant levels of intrinsically disordered structure. Significantly, AR-AF1 (amino acids 142−485) comprises a major part of the predicted natural disordered structure, with four helical regions (*29*) interspersed between regions of disorder (Figure 2A).

The limited amount of secondary structure and relatively long stretches of nonordered sequences suggested that the AR-NTD may be highly structurally flexible. It is known that the presence of particular amino acids predisposes proteins to order or disorder (*34, 35*). The N-terminal and AF1 domains show depletion for amino acids that promote order (i.e., C, W, I, F, and V) and an increase in the number of residues associated with disorder (i.e., A, G, S, Q, and P), compared with the more structured ligand and DNA binding domains of the receptor protein (data not shown). This amino acid bias is characteristic of intrinsic disordered proteins or protein domains.

It has been observed that charge−hydropathy (CH) plots show a linear border separating folded, compact structures from unfolded proteins, with the latter characterized by a relatively high net charge and/or low hydropathy and map above this boundary. Figure 3A shows a CH plot for ordered and disordered proteins and reveals that AR-AF1 falls below the boundary and groups with the ordered set of proteins. The second binary algorithm used to study AR-AF1 structure was the neural trained network, PONDR. This uses several parameters, in addition to net charge, to predict the propensity of each amino acid in the sequence to be ordered or disordered (*35, 36*). A plot of the cumulative distribution frequency (CDF) against the PONDR score also results in a linear boundary between structured and intrinsically disordered proteins (Figure 3B). The CDF curve for AR-AF1 falls below the boundary, indicating a significantly disordered polypeptide (Figure 3B). In contrast, a similar analysis of the AR-DBD-LBD sequence shows a curve above the boundary (data not shown). The discrepancy between the CH and CDF predictions for AR-AF1 is interesting and possibly significant as such differences may reveal information about the ordered and disordered folded state of the native protein. Proteins predicted to be disordered by CDF analysis and ordered by the CH plot have been suggested to have properties consistent with a dynamic conformation and to fall into a "collapsed disorder class" of proteins, typical of the molten globule folding intermediate (*35, 44*).

Interactions of AR-AF1 with 8-Anilinonaphthalene-1-sulfonic Acid. The results of the bioinformatic analyses described above are in good agreement with our previous circular dichroism, steady state fluorescence, and FTIR spectroscopy analysis of AR-AF1 in buffer, TMAO, hydrophobic solvent, or urea, which indicated that this domain is structurally flexible and can be both stabilized and destabilized in different environments (*29, 32*). However, this analysis also suggests that the AR-AF1 domain may exist in an intermediate folded state that is neither random coil nor fully structured, but similar to a molten or pre-molten

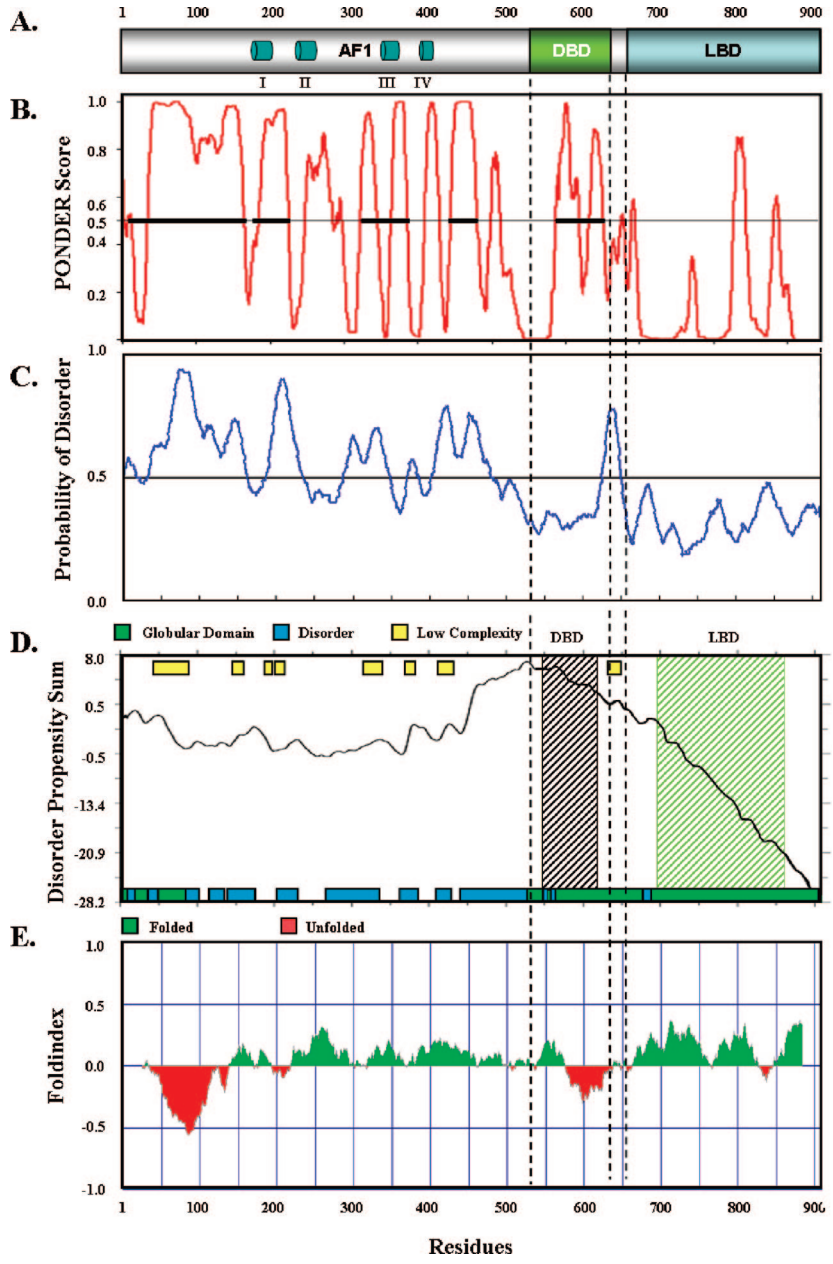

FIGURE 2: Analysis of the primary amino acid sequence of the human androgen receptor. (A) Schematic representation of the domain organization of the AR, showing the ligand (LBD) and DNA (DBD) binding domains and the AF1 transactivation domain. Four α-helical regions previously characterized are highlighted (*29*). (B−E) Predictions of regions of natural disordered sequence are shown using four different algorithms: (B) PONDER plot (*35, 36*), where a score above 0.5 indicates disorder; (C) RONN plot (*39*), where similarly a score above 0.5 indicates disorder; (D) GlobPlot, where disorder propensity is indicated by the upward slops of the curve (*38*); and (E) FoldIndex, where a negative value indicates disordered structure (*40*).

globule conformation. To test this possibility, the interaction of purified AR-AF1 and the hydrophobic probe 8-anilinonaphthalene-1-sulfonic acid (ANS) was investigated by fluorescence spectroscopy. The interaction of ANS with various proteins has been used previously to characterize hydrophobic surfaces and structural conformations (*41, 42, 45, 46*). In aqueous solution, ANS has limited emission spectra when excited at 370 nm, with an emission maximum at 533 nm, but upon interaction with a molten globule folding state or hydrophobic "patch", a dramatic enhancement in emission spectra results with a maximum at 480 nm (*41, 46*). In addition, ANS interacts with the molten globule state, but less well with either fully folded (globular) or unfolded (random coil) protein conformations (*46*).

Purified AR-AF1 was titrated with increasing amounts of ANS which resulted in a hyperbolic curve, and ANS-binding sites appeared saturated above 40 μM (Figure 4A). Incubation of AR-AF1 with ANS resulted in a significant increase in fluorescence intensity and a blue shift for the maximum emission to 465 nm (Figure 4B). Interestingly, the fluorescence intensity was further enhanced in the presence of TMAO but abolished in a urea-rich environment (Figure 4B). Analysis of the ANS binding by the Scatchard method revealed a nonlinear plot and suggested less than or equal to one molecule of ANS bound per AF-1 molecule (data not shown). The observed quenching of tryptophan fluorescence emission by ANS binding further suggested the relative proximity of the ANS binding site to the two tryptophans at

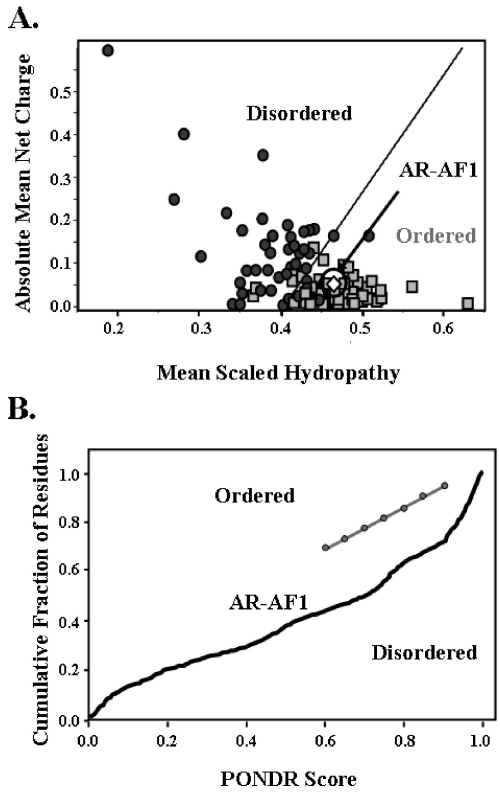

FIGURE 3: Disorder prediction comparisons. (A) Charge−hydropathy (CH) plot showing the position of the AR-AF1 polypeptide (◇) relative to ordered and disordered protein sequences. The solid line indicates the linear boundary between these structural states. (B) Plot of the cumulative fraction of residues vs PONDR scores. The boundary between ordered and disordered sequences (circles) and the plot for AR-AF1 (solid line) are shown.

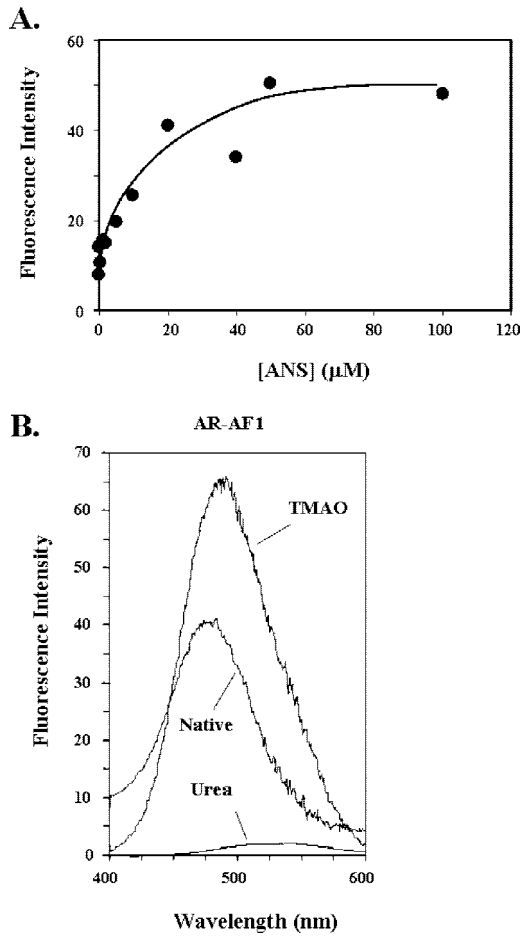

FIGURE 4: ANS−AR-AF1 fluorescence studies. (A) Titration of ANS binding to 1 μM AR-AF1. The increase in ANS fluorescence was measured at 490 nm after excitation at 370 nm. (B) Fluorescence emission spectrum for the ANS−AR-AF1 complex under native conditions, in the presence of urea or the structure-stabilizing osmolyte TMAO. AR-AF1 at a concentration of 1 μM was incubated with 50 μM ANS for 30 min in the dark for each buffer condition, and the formed complexes were excited at 370 nm and the emission spectra measured from 400 to 600 nm.

positions 396 and 432 (data not shown). An extremely well studied protein, which can exist in both molten globule and globular forms, is α-lactalbumin (αLA) (reviewed in ref *47*). The molten globule state can be achieved by decreasing the pH of the solution from pH 7 to 2. Ridged structured proteins show a distinct urea-induced unfolding profile for ANS binding when compared with proteins in a molten globule conformation (*42*). The urea-induced unfolding of AR-AF1 was therefore compared with that of the structured protein BSA and αLA in the molten globule conformation. Figure 5A shows that BSA unfolds cooperatively, with 50% unfolded at 3.7 M urea. In contrast, αLA was significantly more sensitive to urea and showed 50% unfolding at 1.3 M urea and a noncooperative profile (Figure 5A). AR-AF1 was similarly sensitive to urea and unfolded in a noncooperative manner with 50% unfolded at 1.0 M urea (Figure 5B). Taken together, these data indicate that AR-AF1 in a native state binds ANS and exhibits ANS binding characteristics similar to those of a well-characterized molten globule state protein.

Size-Exclusion Chromatography of AR-AF1. Size-exclusion or gel filtration chromatography is a sensitive tool for accurately determining the native molecular mass and hydrodynamic properties of proteins, including the Stokes radius. Recently, this technique has been used for assessing the disorder and structural properties of proteins (*48–52*). To determine the native molecular mass and Stokes radius of AR-AF1, the purified polypeptide was resolved on a column packed with Superose-6 resin. The column was calibrated using standard proteins (albumin, ovalbumin, chymotrypsinogen A, and ribonuclease A) and the void volume ($V_o = 32.5 \pm 0.5$ mL) measured using blue dextran. A calibration curve was generated relating the molecular mass and the hydrodynamic, or Stokes radius, of the standard proteins (data not shown). Purified AR-AF1 (1–2 mg/mL) was resolved under identical conditions, and a representative elution profile and a Coomassie-stained gel of the peak fractions are shown: average elution volume (V_e) for AR-AF1 was calculated to be 57.7 ± 0.6 mL with a gel phase distribution coefficient (K_{av}) of 0.71 (Figure 6A and data not shown). By comparing these values with those of the standard proteins, we calculated the molecular mass and Stokes radius of AR-AF1 to be 64.7 ± 6.4 kDa and 36.4 ± 1.8 Å, respectively (Figure 6B). These values differ greatly from predicted values (Figure 6B) and strongly suggest AR-AF1 is less compact than a native protein similar in size. Uversky and colleagues have recently collated molecular mass and the Stokes radius for a range of proteins and generated "folding-state" curves for globular, unfolded, molten globule, and pre-molten globule proteins (*48, 49, 53*). Therefore, using these data and plotting the molecular masses and Stokes radii for the AR-AF1 domain, we directly compared the properties of AR-AF1 with those of different folding states. Figure 6C shows that the predicted molecular mass and Stokes radius

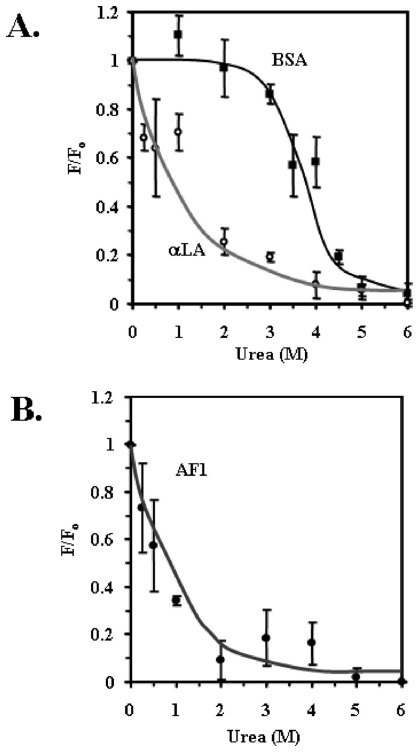

FIGURE 5: Urea-induced unfolding of ANS−protein complexes. (A) ANS−BSA or ANS−α-lactalbumin protein (pH 2) was titrated with increasing amounts of urea. Each protein at a concentration of 1 μM was incubated with 50 μM ANS for 30 min in the dark and challenged with increasing urea concentraions. After excitation at 370 nm, the fluorescence emission in the absence (F_o) and presence of urea (F) was measured at 480 nm. F/F_o was then plotted vs urea concentration. (B) Analysis of ANS−AF1 complexes as described for panel A.

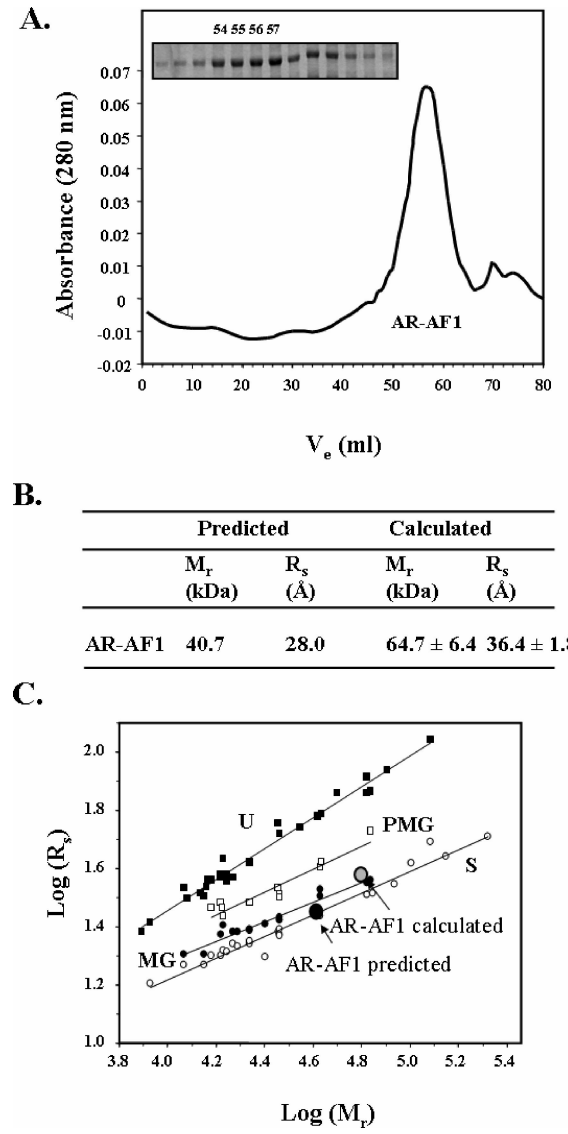

	Predicted		Calculated	
	M_r (kDa)	R_s (Å)	M_r (kDa)	R_s (Å)
AR-AF1	40.7	28.0	64.7 ± 6.4	36.4 ± 1.8

FIGURE 6: Size-exclusion chromatography of native AR-AF1. (A) A representative elution profile (absorbance at 280 nm) for AR-AF1 on a Superose-6 column. The inset shows a representative Coomassie-stained gel of peak fractions. (B) Predicted (from primary amino acid sequence) and experimental values (calculated) for AR-AF1 molecular mass and Stokes radius. (C) Comparison of the predicted and actual partition parameters [molecular mass (M_r) and Stokes radius (R_s)] with published data (*48, 49*) for proteins representing unfolded (U), pre-molten globule (PMG), molten globule (MG), and structured (S) conformational states.

for AR-AF1 are positioned on the folding curve for a globular structured protein, but the experimental calculated properties for AR-AF1 place the receptor transactivation domain with proteins in a molten globule state. Taken together with the ANS binding experiments and computational analysis, these results suggest that the native structure of AR-AF1 has properties of a protein in a pre-molten globule or molten globule state and distinct from a globular or a random coil conformation.

DISCUSSION

Recently published evidence supports the hypothesis that the N-terminal transactivation domain of the AR and other SHRs is significantly disordered and undergoes an induced folding upon protein–protein interactions. However, an important question is the conformation of the native AR-AF1 domain. To gain insight into this, we have used a combination of computational and experimental analysis of the isolated AR-AF1 domain. Proteins can be thought to exist in conformational states distinct from a stable folded (ordered) or fully unfolded (extended disordered) structure sometimes termed collapsed disordered structure (*35, 54*). This can be illustrated by the following scheme: U ↔ PG ↔ MG ↔ S, where U is fully unfolded, PG and MG represent the collapsed disorder conformation and represent intermediates with increasing amounts of stabilized interactions, termed pre-molten globule or molten globule, and S is the structured folded conformation. The data presented provide several lines of evidence that the native AR-AF1 domain is neither fully random coil nor a stable globular conformation but has properties reminiscent of partially folded protein intermediates.

First, the differences in disorder prediction studies suggest a dynamic structure similar to the molten globule state. RONN, GlobPlot, and CDF (PONDR) all predict significant regions of natural disordered structure within AR-NTD/AF1. In contrast, analysis of charge−hydropathy parameters suggests less disorder and groups the AR-NTD/AF1 with ordered proteins. These predictive algorithms, while using information from protein structure databases in the case of PONDR, RONN, and GlobPlot, use different comparative parameters to classify amino acids or a sequence as likely to be ordered or disordered (*34–40*). Contrasting findings from CH and CDF have previously been noted and suggested

to indicate an intermediate folded state distinct from extended disorder and fully folded (*35, 44*).

Second, the fluorescence properties of complexes between AR-AF1 and the hydrophobic probe ANS suggest a partially folded intermediate resembling a pre-molten globule or molten globule state. ANS exhibits little fluorescence in aqueous solution and limited binding to ridged globular structures or fully unfolded random coils. Upon binding to AR-AF1, ANS showed a significant increase in fluorescence and a blue shift in peak wavelength. A similar blue shift was observed with ANS binding to α-lactalbumin at pH 2, which is in a well-characterized molten globule conformation (data not shown). In agreement with this, the loss of ANS fluorescence upon urea-induced unfolding was essentially the same for AR-AF1 and α-lactalbumin and distinct from the cooperative unfolding observed for a ridged structured protein BSA. Similar analysis was used successfully to characterize the structural properties of a series of different proteins (*41*) and more recently the molten globule-like state of clusterin, a heterodimeric secreted protein of poorly defined function (*42*), and α-crystallin (*45*). Three regions of predicted disorder were observed for the α-subunit (C-terminus) and β-subunit (N-terminus) of clusterin, and urea treatment of ANS−clusterin complexes revealed unfolding properties similar to those of α-lactalbumin and apomyoglobulin, both in a molten globule conformation. Therefore, analysis of a number of ANS−protein binding properties can be used to describe the structural properties of proteins, and for the AR-AF1 domain, these studies supported a structural state resembling the collapsed disordered conformation.

Third, gel filtration chromatography has been used to characterize the folded conformations of proteins as it was noted the hydrodynamic properties of polypeptides can be related to conformation (*48, 49, 55*). Analysis of the native AR-AF1 revealed a protein with a molecular mass and a Stokes radius significantly higher than those predicted from amino acid sequence. Using the data sets published by Uversky and co-workers (*48, 49*), it was possible to compare the gel permeability properties of AR-AF1 with those of proteins in different conformational states: extended disorder (random coil), collapsed disorder (pre-molten globule or molten globule), and folded globular (structured). While the theoretical properties of AR-AF1 place the receptor transactivation domain with the structured proteins, the experimental data group AF1 with the molten globule conformational state. Taken together, the findings from computational and experiential studies suggest that AR-AF1 exists in a conformational state distinct from random coil and a stable folded structure, consistent with the pre-molten globule or molten globule-like structure.

Fourth, the findings for the isolated AR-AF1 domain are likely to be meaningful and not a consequence of using the isolated polypeptide. The isolated transactivation has been shown to activate transcription in a manner similar to that of the full-length receptor (see refs *9*, *10*, and *12*). Furthermore, bioinformatic analysis of the full-length AR, AR-NTD, or AF1 sequences, together with spectroscopy and limited proteolysis studies of the AR-NTD and AR-AF1, gives essentially identical results (ref *29*, this study, and manuscript in preparation). However, it is worth noting that studies with the ER, GR, and PR have emphasized a role for interdomain interactions, and/or DNA binding, which are likely to influence the function and structure of the intact receptor protein (see refs *7*, *33*, and *56* and references therein).

Protein–protein interactions have been shown to induce and/or stabilize secondary and tertiary structure within the isolated AF1 transactivation domain or NTD of the AR (*29, 32*), GR (*28, 31, 56*), and ERα (*30*). The binding of a coregulatory protein termed JDP-2 (Jun dimerization protein 2) to the PR DBD resulted in an increase in the level of α-helical structure in the NTD, as a consequence of interdomain communication (*33*). In this study, we show that folding of the AR-AF1 domain into a protease resistant conformation is achieved with two different specific binding partners (RAP74, a subunit of TFIIF and SRC-1a), but not a noninteracting polypeptide. An interesting question is whether the structure induced is similar for all protein–protein interactions or if the AF1 domain can adopt different conformations depending on the binding partner. While a definitive answer awaits more detailed structural analysis, it is interesting to note that both RAP74 polypeptides and SRC-1a (Peptide B) lead to similar patterns of protected fragments with the major effect being a protease resistant conformation in full-length AR-AF1. As a similar pattern of protection is observed with both the chemical chaperone TMAO and a short 40-amino acid peptide, it seems likely the protease resistance is not simply the result of the binding partners occluding the cleavage sites but involves a conformational change within the AR-AF1 domain. Protease resistance and an induced α-helical conformation have previously been observed with the CTD of RAP74 (*29, 32*).

To date, only structures for the isolated LBD and DBD of nuclear receptors have been reported. This structural analysis of AR-NTD/AF1 has emphasized the limited secondary structure content and regions of intrinsic disorder. However, the prediction of natural disordered structure does not necessarily mean random coil (see refs *13*, *35*, and *55*). There are a number of advantages in the AF1 domain being structurally plastic, in contrast to the stable folded structures of the LBD and DBD. These include maintaining specificity in multiple protein–protein interactions, without the need for high affinities (*57*), an increased contact surface for individual interactions, and permitting access for different modifying enzymes, such as kinases (phosphorylation) and ligases (summoylation) (reviewed in ref *13*). In the study presented here, we demonstrate that native AR-AF1 has structural properties characteristic of a collapsed disordered conformation, which has been called a pre-molten globule or molten globule state. This is likely to have important implications for AR function on androgen-regulated genes.

ACKNOWLEDGMENT

We are grateful to colleagues who attended the 2006 FASEB Summer Conference on the Dynamic Structure of the Nuclear Hormone Receptor for helpful discussion on the studies reported.

REFERENCES

1. Poujol, N., Wurtz, J. M., Tahiri, B., Lumbroso, S., Nicolas, J. C., Moras, D., and Sultan, C. (2000) Specific Recognition of Androgens by their Nuclear Receptor. A Structure-Function Study. *J. Biol. Chem. 275*, 24022–24031.
2. Matias, P. M., Donner, P., Coelho, R., Thomaz, M., Peixoto, C., Macedo, S., Otto, N., Joschko, S., Scholz, P., Wegg, A., Basler,

S., Schafer, M., Egner, U., and Carrondo, M. A. (2000) Structural Evidence for Ligand Specificity in the Binding Domain of the Human Androgen Receptor. Implications for Pathogenic Gene Mutations. *J. Biol. Chem. 275*, 26164–26171.
3. Sack, J. S., Kish, K. F., Wang, C., Attar, R. M., Kiefer, S. E., An, Y., Wu, G. Y., Scheffler, J. E., Salvati, M. E., Krystek, S. R., Jr., Weinmann, R., and Einspahr, H. M. (2001) Crystallographic Structures of the Ligand-Binding Domains of the Androgen Receptor and its T877A Mutant Complexed with the Natural Agonist Dihydrotestosterone. *Proc. Natl. Acad. Sci. U.S.A. 98*, 4904–4909.
4. Bohl, C. E., Wu, Z., Miller, D. D., Bell, C. E., and Dalton, J. T. (2007) Crystal Structure of the T877A Human Androgen Receptor Ligand-Binding Domain Complexed to Cyproterone Acetate Provides Insight for Ligand-Induced Conformational Changes and Structure-Based Drug Design. *J. Biol. Chem. 282*, 13648–13655.
5. He, B., Gampe, R. T., Jr., Kole, A. J., Hnat, A. T., Stanley, T. B., An, G., Stewart, E. L., Kalman, R. I., Minges, J. T., and Wilson, E. M. (2004) Structural Basis for Androgen Receptor Interdomain and Coactivator Interactions Suggests a Transition in Nuclear Receptor Activation Function Dominance. *Mol. Cell 16*, 425–438.
6. Shaffer, P. L., Jivan, A., Dollins, D. E., Claessens, F., and Gewirth, D. T. (2004) Structural Basis of Androgen Receptor Binding to Selective Androgen Response Elements. *Proc. Natl. Acad. Sci. U.S.A. 101*, 4758–4763.
7. Lavery, D. N., and McEwan, I. J. (2005) Structure and Function of Steroid Receptor AF1 Transactivation Domains: Induction of Active Conformations. *Biochem. J. 391*, 449–464.
8. Simental, J. A., Sar, M., Lane, M. V., French, F. S., and Wilson, E. M. (1991) Transcriptional activation and nuclear targeting signals of the human androgen receptor. *J. Biol. Chem. 266*, 510–518.
9. Jenster, G., van der Korput, H. A., Trapman, J., and Brinkmann, A. O. (1995) Identification of two transcription activation units in the N-terminal domain of the human androgen receptor. *J. Biol. Chem. 270*, 7341–7346.
10. Chamberlain, N. L., Whitacre, D. C., and Miesfeld, R. L. (1996) Delineation of two distinct type 1 activation functions in the androgen receptor amino-terminal domain. *J. Biol. Chem. 271*, 26772–26778.
11. McEwan, I. J., and Gustafsson, J. (1997) Interaction of the Human Androgen Receptor Transactivation Function with the General Transcription Factor TFIIF. *Proc. Natl. Acad. Sci. U.S.A. 94*, 8485–8490.
12. Reid, J., Murray, I., Watt, K., Betney, R., and McEwan, I. J. (2002) The Androgen Receptor Interacts with Multiple Regions of the Large Subunit of General Transcription Factor TFIIF. *J. Biol. Chem. 277*, 41247–41253.
13. Dunker, A. K., Brown, C. J., Lawson, J. D., Iakoucheva, L. M., and Obradovic, Z. (2002) Intrinsic Disorder and Protein Function. *Biochemistry 41*, 6573–6582.
14. Dyson, H. J., and Wright, P. E. (2005) Intrinsically Unstructured Proteins and their Functions. *Nat. Rev. Mol. Cell Biol. 6*, 197–208.
15. Donaldson, L. J., and Cavanagh, J. (1992) Clinical Complaints and their Handling: A Time for Change? *Qual. Health Care 1*, 21–25.
16. O'Hare, P., and Williams, G. (1992) Structural Studies of the Acidic Transactivation Domain of the Vmw65 Protein of Herpes Simplex Virus using ^{1}H NMR. *Biochemistry 31*, 4150–4156.
17. Shen, F., Triezenberg, S. J., Hensley, P., Porter, D., and Knutson, J. R. (1996) Transcriptional Activation Domain of the Herpesvirus Protein VP16 Becomes Conformationally Constrained upon Interaction with Basal Transcription Factors. *J. Biol. Chem. 271*, 4827–4837.
18. Uesugi, M., Nyanguile, O., Lu, H., Levine, A. J., and Verdine, G. L. (1997) Induced Alpha Helix in the VP16 Activation Domain upon Binding to a Human TAF. *Science 277*, 1310–1313.
19. Jonker, H. R., Wechselberger, R. W., Boelens, R., Folkers, G. E., and Kaptein, R. (2005) Structural Properties of the Promiscuous VP16 Activation Domain. *Biochemistry 44*, 827–839.
20. Lee, H., Mok, K. H., Muhandiram, R., Park, K. H., Suk, J. E., Kim, D. H., Chang, J., Sung, Y. C., Choi, K. Y., and Han, K. H. (2000) Local Structural Elements in the mostly Unstructured Transcriptional Activation Domain of Human p53. *J. Biol. Chem. 275*, 29426–29432.
21. Schmitz, M. L., dos Santos Silva, M. A., Altmann, H., Czisch, M., Holak, T. A., and Baeuerle, P. A. (1994) Structural and Functional Analysis of the NF-κB p65 C Terminus. An Acidic and Modular Transactivation Domain with the Potential to Adopt an α-Helical Conformation. *J. Biol. Chem. 269*, 25613–25620.
22. Radhakrishnan, I., Perez-Alvarado, G. C., Parker, D., Dyson, H. J., Montminy, M. R., and Wright, P. E. (1997) Solution Structure of the KIX Domain of CBP Bound to the Transactivation Domain of CREB: A Model for Activator:Coactivator Interactions. *Cell 91*, 741–752.
23. Hua, Q. X., Jia, W. H., Bullock, B. P., Habener, J. F., and Weiss, M. A. (1998) Transcriptional Activator-Coactivator Recognition: Nascent Folding of a Kinase-Inducible Transactivation Domain Predicts its Structure on Coactivator Binding. *Biochemistry 37*, 5858–5866.
24. Radhakrishnan, I., Perez-Alvarado, G. C., Parker, D., Dyson, H. J., Montminy, M. R., and Wright, P. E. (1999) Structural Analyses of CREB-CBP Transcriptional Activator-Coactivator Complexes by NMR Spectroscopy: Implications for Mapping the Boundaries of Structural Domains. *J. Mol. Biol. 287*, 859–865.
25. Dahlman-Wright, K., Baumann, H., McEwan, I. J., Almlof, T., Wright, A. P., Gustafsson, J. A., and Hard, T. (1995) Structural Characterization of a Minimal Functional Transactivation Domain from the Human Glucocorticoid Receptor. *Proc. Natl. Acad. Sci. U.S.A. 92*, 1699–1703.
26. Baskakov, I. V., Kumar, R., Srinivasan, G., Ji, Y. S., Bolen, D. W., and Thompson, E. B. (1999) Trimethylamine N-Oxide-Induced Cooperative Folding of an Intrinsically Unfolded Transcription-Activating Fragment of Human Glucocorticoid Receptor. *J. Biol. Chem. 274*, 10693–10696.
27. Zor, T., Mayr, B. M., Dyson, H. J., Montminy, M. R., and Wright, P. E. (2002) Roles of Phosphorylation and Helix Propensity in the Binding of the KIX Domain of CREB-Binding Protein by Constitutive (c-Myb) and Inducible (CREB) Activators. *J. Biol. Chem. 277*, 42241–42248.
28. Kumar, R., Lee, J. C., Bolen, D. W., and Thompson, E. B. (2001) The Conformation of the Glucocorticoid Receptor af1/tau1 Domain Induced by Osmolyte Binds Co-Regulatory Proteins. *J. Biol. Chem. 276*, 18146–18152.
29. Reid, J., Kelly, S. M., Watt, K., Price, N. C., and McEwan, I. J. (2002) Conformational Analysis of the Androgen Receptor Amino-Terminal Domain Involved in Transactivation. Influence of Structure-Stabilizing Solutes and Protein-Protein Interactions. *J. Biol. Chem. 277*, 20079–20086.
30. Warnmark, A., Wikstrom, A., Wright, A. P., Gustafsson, J. A., and Hard, T. (2001) The N-Terminal Regions of Estrogen Receptor α and β are Unstructured in Vitro and show Different TBP Binding Properties. *J. Biol. Chem. 276*, 45939–45944.
31. Kumar, R., Volk, D. E., Li, J., Lee, J. C., Gorenstein, D. G., and Thompson, E. B. (2004) TATA Box Binding Protein Induces Structure in the Recombinant Glucocorticoid Receptor AF1 Domain. *Proc. Natl. Acad. Sci. U.S.A. 101*, 16425–16430.
32. Kumar, R., Betney, R., Li, J., Thompson, E. B., and McEwan, I. J. (2004) Induced α-Helix Structure in AF1 of the Androgen Receptor upon Binding Transcription Factor TFIIF. *Biochemistry 43*, 3008–3013.
33. Wardell, S. E., Kwok, S. C., Sherman, L., Hodges, R. S., and Edwards, D. P. (2005) Regulation of the Amino-Terminal Transcription Activation Domain of Progesterone Receptor by a Cofactor-Induced Protein Folding Mechanism. *Mol. Cell. Biol. 25*, 8792–8808.
34. Romero, P., Obradovic, Z., Li, X., Garner, E. C., Brown, C. J., and Dunker, A. K. (2001) Sequence Complexity of Disordered Protein. *Proteins 42*, 38–48.
35. Oldfield, C. J., Cheng, Y., Cortese, M. S., Brown, C. J., Uversky, V. N., and Dunker, A. K. (2005) Comparing and Combining Predictors of Mostly Disordered Proteins. *Biochemistry 44*, 1989–2000.
36. Li, X., Romero, P., Rani, M., Dunker, A. K., and Obradovic, Z. (1999) Predicting Protein Disorder for N-, C-, and Internal Regions. *Genome Inf. Ser., v10 1999,* 30–40.
37. Kyte, J., and Doolittle, R. F. (1982) A Simple Method for Displaying the Hydropathic Character of a Protein. *J. Mol. Biol. 157*, 105–132.
38. Linding, R., Russell, R. B., Neduva, V., and Gibson, T. J. (2003) GlobPlot: Exploring Protein Sequences for Globularity and Disorder. *Nucleic Acids Res. 31*, 3701–3708.
39. Yang, Z. R., Thomson, R., McNeil, P., and Esnouf, R. M. (2005) RONN: The Bio-Basis Function Neural Network Technique Applied to the Detection of Natively Disordered Regions in Proteins. *Bioinformatics 21*, 3369–3376.
40. Prilusky, J., Felder, C. E., Zeev-Ben-Mordehai, T., Rydberg, E. H., Man, O., Beckmann, J. S., Silman, I., and Sussman, J. L. (2005)

FoldIndex: A Simple Tool to Predict Whether a Given Protein Sequence is Intrinsically Unfolded. *Bioinformatics 21*, 3435–3438.

41. Cardamone, M., and Puri, N. K. (1992) Spectrofluorimetric Assessment of the Surface Hydrophobicity of Proteins. *Biochem. J. 282* (2), 589–593.
42. Bailey, R. W., Dunker, A. K., Brown, C. J., Garner, E. C., and Griswold, M. D. (2001) Clusterin, a Binding Protein with a Molten Globule-like Region. *Biochemistry 40*, 11828–11840.
43. Kumar, R., Serrette, J. M., and Thompson, E. B. (2005) Osmolyte-Induced Folding Enhances Tryptic Enzyme Activity. *Arch. Biochem. Biophys. 436*, 78–82.
44. Haag Breese, E., Uversky, V. N., Georgiadis, M. M., and Harrington, M. A. (2006) The Disordered Amino-Terminus of SIMPL Interacts with Members of the 70-kDa Heat-Shock Protein Family. *DNA Cell Biol. 25*, 704–714.
45. Sharma, K. K., Kaur, H., Kumar, G. S., and Kester, K. (1998) Interaction of 1,1′-Bi(4-Anilino)Naphthalene-5,5′-Disulfonic Acid with α-Crystallin. *J. Biol. Chem. 273*, 8965–8970.
46. Semisotnov, G. V., Rodionova, N. A., Razgulyaev, O. I., Uversky, V. N., Gripas', A. F., and Gilmanshin, R. I. (1991) Study of the "Molten Globule" Intermediate State in Protein Folding by a Hydrophobic Fluorescent Probe. *Biopolymers 31*, 119–128.
47. Kuwajima, K. (1996) The Molten Globule State of α-Lactalbumin. *FASEB J. 10*, 102–109.
48. Uversky, V. N. (1993) Use of Fast Protein Size-Exclusion Liquid Chromatography to Study the Unfolding of Proteins which Denature through the Molten Globule. *Biochemistry 32*, 13288–13298.
49. Tcherkasskaya, O., and Uversky, V. N. (2001) Denatured Collapsed States in Protein Folding: Example of Apomyoglobin. *Proteins 44*, 244–254.
50. Denning, D. P., Uversky, V., Patel, S. S., Fink, A. L., and Rexach, M. (2002) The *Saccharomyces cerevisiae* Nucleoporin Nup2p is a Natively Unfolded Protein. *J. Biol. Chem. 277*, 33447–33455.
51. Naseem, F., Ahmad, B., Ashraf, M. T., and Khan, R. H. (2004) Molten Globule-Like Folding Intermediate of Asialofetuin at Acidic pH. *Biochim. Biophys. Acta 1699*, 191–199.
52. Carvalho, A. F., Costa-Rodrigues, J., Correia, I., Costa Pessoa, J., Faria, T. Q., Martins, C. L., Fransen, M., Sa-Miranda, C., and Azevedo, J. E. (2006) The N-Terminal Half of the Peroxisomal Cycling Receptor Pex5p is a Natively Unfolded Domain. *J. Mol. Biol. 356*, 864–875.
53. Uversky, V. N. (2002) What does it Mean to be Natively Unfolded? *Eur. J. Biochem. 269*, 2–12.
54. Christensen, H., and Pain, R. H. (1991) Molten Globule Intermediates and Protein Folding. *Eur. Biophys. J. 19*, 221–229.
55. Receveur-Brechot, V., Bourhis, J. M., Uversky, V. N., Canard, B., and Longhi, S. (2006) Assessing Protein Disorder and Induced Folding. *Proteins 62*, 24–45.
56. Kumar, R., Baskakov, I. V., Srinivasan, G., Bolen, D. W., Lee, J. C., and Thompson, E. B. (1999) Interdomain Signaling in a Two-Domain Fragment of the Human Glucocorticoid Receptor. *J. Biol. Chem. 274*, 24737–24741.
57. Lavery, D. N., and McEwan, I. J. (2008) Functional characterization of the native NH_2-terminal transactivation domain of the human androgen receptor: Binding kinetics for interactions with TFIIF and SRC-1a. *Biochemistry 47*, 3352–3359.

BI702221E